Dalton Transactions

Accepted Manuscript

ROYAL SOCIETY OF CHEMISTRY

www.rsc.org/dalton

TOC Graphic

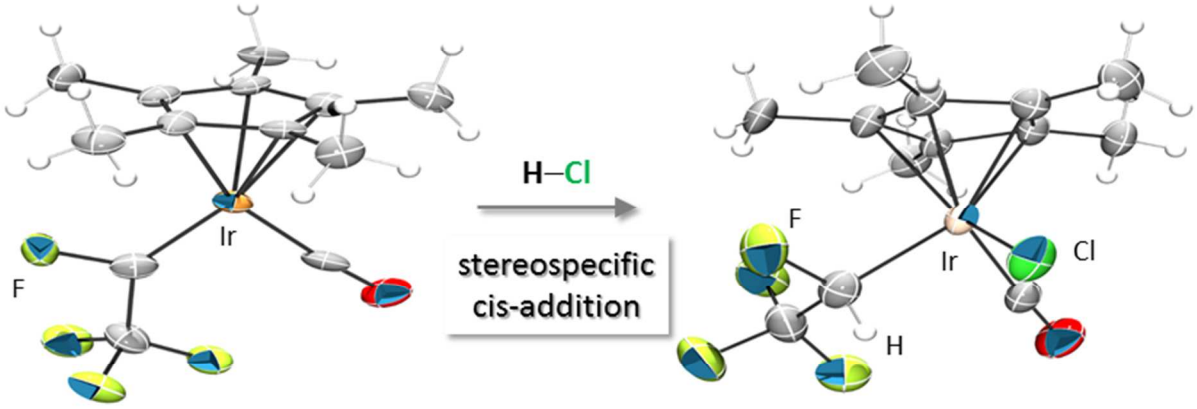

Addition of HCl to perfluorocarbene complexes of iridium occurs regiospecifically and stereospecifically.

Synthesis, Structure, and Reactivity of Iridium Perfluorocarbene Complexes: Regio- and Stereo-specific Addition of HCl Across a Metal Carbon Double Bond.

Jian Yuan,[#] *Cheryl J. Bourgeois,*[#] *Arnold L. Rheingold*[§]*, Russell P. Hughes,**[#]

Department of Chemistry, 6128 Burke Laboratory, Dartmouth College, Hanover, New Hampshire 03755 and Department of Chemistry, University of California, San Diego, California 92093-0358

rph@dartmouth.edu

RECEIVED DATE

[#] Dartmouth College

[§] University of California, San Diego

Abstract: Reductive activation of an α-fluorine in the perfluoroalkyl complexes Cp*(L)(I)Ir-CF_2R_F using Mg/graphite leads to perfluorocarbene complexes Cp*(L)Ir=CFR_F (L= CO, PMe_3; R_F = CF_3, C_2F_5, C_6F_5). New complexes E-Cp*(PMe_3)Ir=CFC_2F_5 and E-Cp*(CO)Ir=CFC_6F_5 have been characterized by single crystal X-ray diffraction studies, and a comparison of metric parameters with previously reported analogues is reported. Experimental NMR and computational DFT (B3LYP/LACV3P**++) studies agree that for Ir=CFR_F complexes (R_F = CF_3, CF_2CF_3) the thermodynamic preference for the E or Z isomer depends on the steric requirements of ligand L; when

L=CO the Z-isomer (F cis to Cp*) is preferred and for L= PMe_3 the E-isomer is preferred. When reduction of the precursors is carried out in the dark the reaction is completely selective to produce E- or Z-isomers. Exposure of solutions of these compounds to ambient light results in slow conversion to a photostationary non-equilibrium mixture of E and Z isomers. In the dark, these E/Z mixtures convert thermally to their preferred E or Z equilibrium geometries in an even slower reaction. A study of the temperature dependent kinetics of this dark transformation allows $\Delta G^{\ddagger}_{298}$ for rotation about the Ir=$CFCF_3$ double bond to be experimentally determined as 27 kcal/mol; a DFT/B3LYP/LACV3P**++ calculation of this rotation barrier is in excellent agreement (29 kcal/mol) with the experimental value. Reaction of HCl with toluene solutions of Cp*(L)Ir=CFR_F (L = CO , PMe_3) or Cp*(CO)Ir=$C(CF_3)_2$ at low temperature resulted in regiospecific addition of HCl across the metal carbon double bond, ultimately yielding Cp*(L)Ir($CHFR_F$)Cl and Cp*(CO)Ir[$CH(CF_3)_2$]Cl, which have been characterized crystallographically, spectroscopically, and computationally. Reaction of HCl with single E or Z diastereomers of Cp*(L)Ir=CFR_F gives stereospecific cis-addition to give single diastereomers of Cp*Ir(L)($CHFR_F$)Cl; addition of HCl to several different E/Z ratios of Cp*LIr=CFR_F affords ratios of diastereomeric products Cp*(L)Ir($CHFR_F$)Cl identical to the original ratio of starting material isomers. The addition of HCl is therefore demonstrated to be unambiguously regio- and stereo-specific. The observed product regiochemistry of addition of HCl to Ir=CF_2, Ir=CFR_F, and Ir=$C(CF_3)_2$ ligands is the same and is not dependent on the ground state energy preference (singlet or triplet) for the free perfluorocarbene. DFT calculations on model HCl addition reactions indicate that this regiochemistry is strongly preferred thermodynamically, but predict that in $H^{\delta+}$-$Cl^{\delta-}$ addition to Cp(PH_3)Ir=CF_2, $H^{\delta+}$ attack at Ir has a lower energy transition state, while for Cp(PH_3)Ir=$CFCF_3$ and Cp(PH_3)Ir=$C(CF_3)_2$, $H^{\delta+}$ attack at C is the kinetically preferred pathway. The carbene carbon atoms in Ir=$CFCF_3$ and Ir=$C(CF_3)_2$ complexes are unambiguously basic towards HCl, while in the Ir=CF_2 analogues the carbene carbon is less basic than its Ir partner, and the eventual regiochemistry of HCl addition arises from thermodynamic control.

Introduction

Complexes with transition-metal carbon double bonds are well known and are extremely useful for a number of synthetic and catalytic applications, most notably in the metathesis reactions of alkenes.[1, 2] The bonding and chemical reactivity of these heteronuclear double bonds have been subjects of considerable discussion; metal carbene complexes have been characterized as nucleophilic (Schrock type) or electrophilic (Fischer type), based on their chemistry with electrophile/nucleophile combinations. Whether these compounds should be referred to as metal-carbene or metal-alkylidene compounds is also part of this bonding discussion, and is sometimes ambiguous. The compounds all formally contain a carbon-heteroatom(metal) double bond, which, depending on the metal, its oxidation state, ancillary ligands, and heteroatoms on the carbene carbon, can be represented by differently weighted combinations of the resonance forms shown in Scheme 1. Generally, electrophilic Fischer type carbene complexes contain at least one heteroatom (usually O or N) on the α-carbon of the carbene ligand, leading to greater contributions from resonance forms **C** and **D** (Scheme 1) and a greater tendency to electrophilic reactivity at the carbene carbon atom. Schrock type compounds are thought to be best represented by resonance forms **A** and **B**, with resultant nucleophilic carbene reactivity. In general, Fischer carbene complexes are viewed as involving a donor/acceptor interaction between a singlet carbene and an empty metal orbital, with backbonding from a filled metal-d into the empty singlet carbene p-orbital, while Schrock carbene complexes are thought to be better represented as forming the double bond by interactions between a triplet carbene and orbitals containing two unpaired metal electrons. It has been suggested that free carbenes that are ground state singlets tend to form Fischer type complexes and those that are ground state triplets tend to form Schrock type systems.[3] The metal-carbon bonding and rationalizations for the Schrock/Fischer designations have been extensively discussed and summarized.[4-7] In this paper we will refer to all these kinds of compounds containing carbene ligands consistently as carbene-metal compounds.

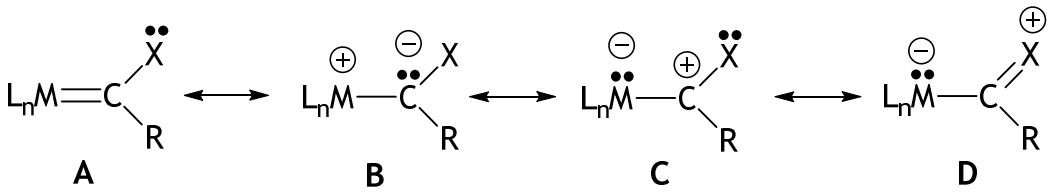

Scheme 1

The structure and reactivity of fluorinated ligands typically vary significantly from their hydrocarbon counterparts,[8, 9] but the effect of fluorine as a carbene substituent (X) in such complexes is not so easily predicted.[10] As the most electronegative element, resonance form **B** would be inductively stabilized, but fluorine is also an excellent π-donor to carbon,[11] leading to stabilization of resonance form **D**. In contrast, a perfluoroalkyl substituent (R_F) such as CF_3 is not a π-donor, but is a strong σ-electron withdrawing group and a π-acceptor via negative hyperconjugation into the C-F σ*-antibonding orbitals,[11-16] both effects resulting in stabilization of resonance form **B**. Free difluorocarbene is a ground state singlet, with a triplet state almost 57 kcal/mol higher in energy,[17-19] changing one fluorine for a CF_3 group to give fluoro(trifluoromethyl)carbene lowers the singlet-triplet energy gap to approximately 9 kcal/mol with the singlet still lower in energy,[20] and replacing the second fluorine with CF_3 to give bis(trifluoromethyl)carbene results in a ground state triplet, calculated to be 18 kcal/mol more stable than its singlet excited state.[17, 20] So, at first blush, we might expect metal complexes of CF_2 and $CF(CF_3)$ to favor Fischer type behavior, while those of $C(CF_3)_2$ should favor the Schrock type reactivity pattern. However these reactivity motifs also depend strongly on the metal, its oxidation state and ancillary ligands.

Reaction regiochemistry is crucial to such reaction characterization for addition of electrophile/nucleophile combinations; the location in the product of the electrophilic and nucleophilic components of the reactant are often used to define the electrophilic or nucleophilic nature of the carbene carbon. Such additions to half sandwich carbene compounds has been explored by several groups. For example, addition of HCl to compounds **1** (Scheme 2) (R = Me, Ph, ^{i}Pr),[21, 22] afforded addition products **2** consistent with the carbene carbon being nucleophilic.

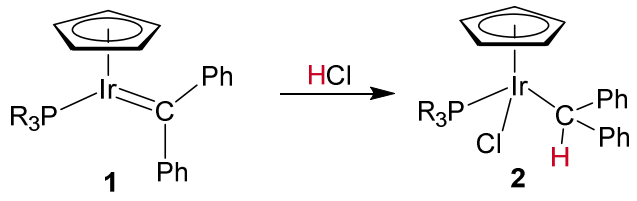

Scheme 2

However, the carbene carbon in rhenium compound **3** appears to be amphiphilic, reacting with nucleophilic phosphines to afford **4a**, but with HCl or HBr to give regioselective formation of compounds **4b** (Scheme 3).[23, 24] Stereochemical information was obtained using the tethered carbene compound **5**,[25] which added HX (X = Cl, Br) to give **6** via a stereoselective cis-addition across the double bond. While the regiochemistry of the HX reactions suggests a nucleophilic carbene carbon, the authors caution that this reaction could also occur by initial protonation at the metal followed by H-migration to carbon.[25] Such apparently amphiphilic behavior of a CF_2 ligand was reported by Roper, who demonstrated that $Ru(CO)_2(PPh_3)_2(CF_2)$ reacted with CH_3NH_2 to afford $Ru(CO)_2(PPh_3)_2(CH_3CN)$ by apparent nucleophilic attack of the amine at an electrophilic CF_2 carbon, but reacted with HCl to give $Ru(CO)_2(PPh_3)_2(CF_2H)Cl$, in which the CF_2 carbon implicitly behaves as a nucleophile.[26] However, the kinetic site of protonation is unclear, as pointed out later by Roper;[10] subsequent experiments illustrated that the migration of H from metals to CF_2 ligands are facile in the presence of a halide nucleophile.[27, 28]

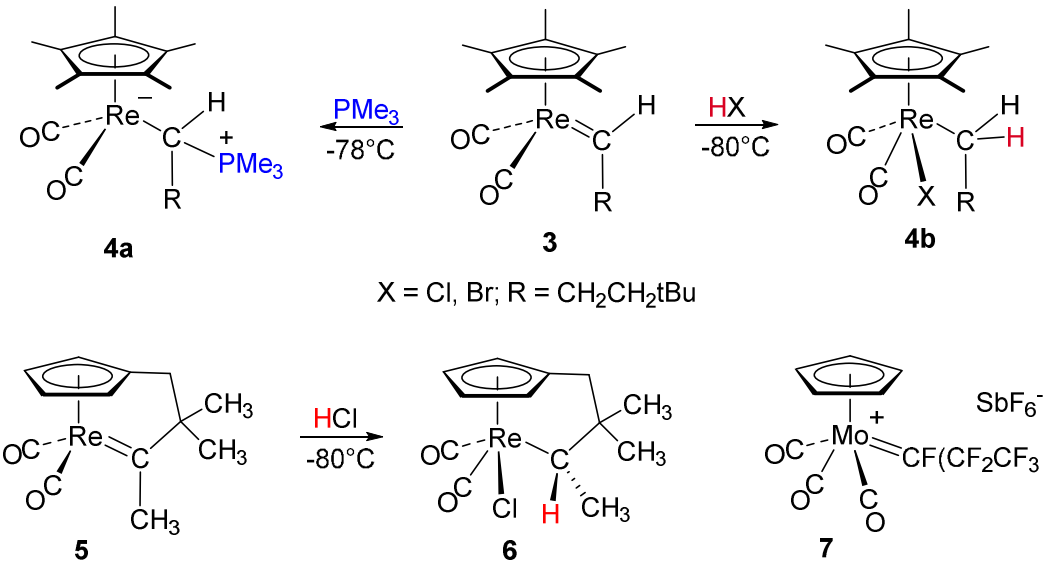

Pioneering work of Roper and his group in the synthesis and characterization of fluorocarbene (and other halocarbene) complexes has been extensively reviewed,[10] but, before our initial forays into this field, only a single report of a perfluoroalkylcarbene complex had appeared. Reger and Dukes reported the preparation of $[Cp(CO)_3Mo{=}CFCF_2CF_3]^+[SbF_6]^-$ (**7**) by addition of SbF_5 in liquid SO_2 to $Cp(CO)_3Mo\text{-}CF_2CF_2CF_3$.[29] This compound was never isolated or studied further and was characterized solely by NMR, although other cationic CF_2 complexes of Mo were isolated and characterized fully.[29, 30]

Study of the addition of HX to perfluorocarbene compounds was a particularly appealing topic for study in our group in view of previous observations for which perfluorocarbene intermediates were proposed. It was found that upon addition of acids HX to solutions of half sandwich compounds $Cp^*(PMe_3)Ir(CF_2R_F)(R)$ **8** (R = H, Me, Ph) in non-polar solvents, α-C-F bond activation occurred with migration of the R group to the α-carbon to ultimately yield exclusively a single diastereomer of $Cp^*(PMe_3)Ir(CF(R_F)(R))(X)$ **9** with the relative stereochemistries at Ir and C shown in Scheme 3.[31-34] In the proposed mechanism, initial α-C-F bond activation by the external acid yields the cationic carbene compound, $[Cp^*(PMe_3)Ir(R)(=C(R_F)(F))]^+$ X^- **10** with loss of HF providing some thermodynamic compensation for breaking the C-F bond.[31, 35] Migration of R to the carbene carbon[36] yields cationic intermediate $[Cp^*(PMe_3)Ir(C(R_F)(F)(R))]^+X^-$ **11**, which is then trapped by anion prior to configurational isomerism at the metal center to yield observed product **9** with the relative stereochemistries shown. These reactions were confirmed to occur under kinetic control[33] and the stereochemistry of the product therefore reflects the preferred stereochemistries of the individual reaction steps. If **10** is indeed an intermediate in this reaction then the kinetic product must arise from a net cis-addition to the E-isomer of the perfluoroalkylcarbene (R_F cis to Cp* as shown in **10**) (or a rather gymnastically spectacular trans-addition to the Z isomer). In addition, the stereochemistry of the Ir=C double bond in **10** must be retained, as must the configuration at Ir in **11** prior to anion trapping. In very polar solvents, such as nitromethane, we have shown that configurational inversion at the metal center of **9** (R=H) does occur via the ion-pair **11**.[33]

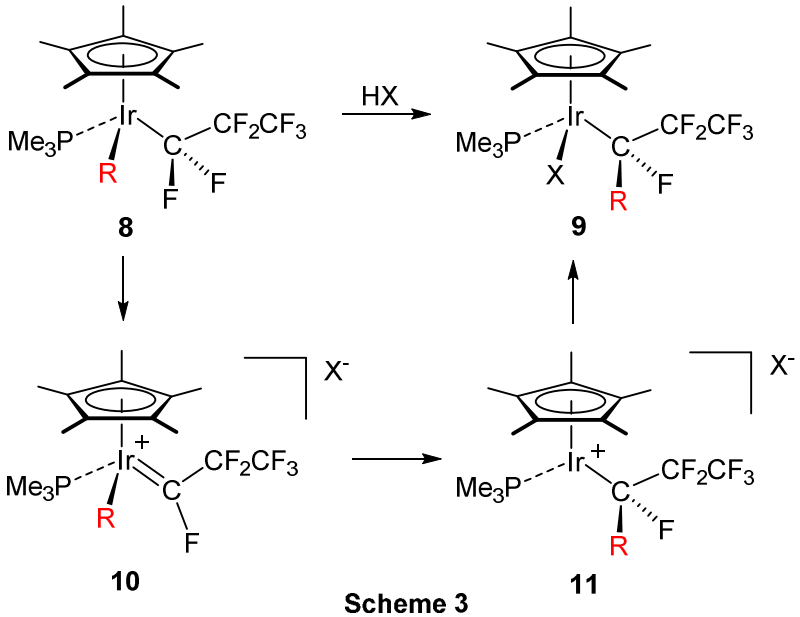

Scheme 3

We have previously reported the synthesis of a novel class of perfluoroalkylcarbene-iridium compounds by reductive activation of iridium perfluoroalkyl iodide precursors.[28, 37] Clearly addition of HX to these double bonds should afford identical compounds **9** (R = H), depending on the regiochemistry of addition. Recently our reductive approach to generation of fluorocarbene ligands from fluoroalkyl ligands has been extended to the formation of much more reactive Cp(L)Co=CFR (R = F, CF_3) analogues.[38, 39]

Here we report more complete studies of these iridium compounds, evaluation of their configurational stabilities under photochemical and thermal conditions, and experimental measurement of the rotation barrier about the Ir=C bond. We also provide an unambiguous demonstration that the addition of HCl to the Ir=C bond occurs in both a regio- and stereospecific manner, and that the regiospecificity does not depend on whether the free fluorocarbene has a singlet or triplet ground state.

Results and Discussion

Preparation and characterization of perfluoroalkylcarbene complexes

The perfluoroalkylcarbene compounds Cp*(L)Ir=CFR_F (L=CO, PMe_3; R_F = CF_3, CF_2CF_3, C_6F_5) **12-16**, can be formed in a facile manner by the action of a number of reducing agents on starting materials of the type, Cp*Ir(L)(CF_2R_F)(I) (L=CO, PMe_3; R_F = CF_3, CF_2CF_3, C_6F_5). Compounds were

produced as variable mixtures of geometric isomers, with the higher priority α-F group *syn* (Z) or *anti* (E) to the higher priority Cp* ligand; factors influencing this E/Z ratio are presented in more detail later. The preparation and crystallographic characterization of E-Cp*(PMe_3)Ir=$CFCF_3$ **13a**,[28] and Z-Cp*(CO)Ir=$CFCF_2CF_3$ **14b**[37] have been previously communicated as have the structures of the parent CF_2 analogues **17**[37] and **18**.[28] *We note with apologies that in a previous communication*[37] *the relative stereochemistries of the E- and Z-isomers of Cp*(CO)Ir=CFCF₃ were incorrectly assigned.*

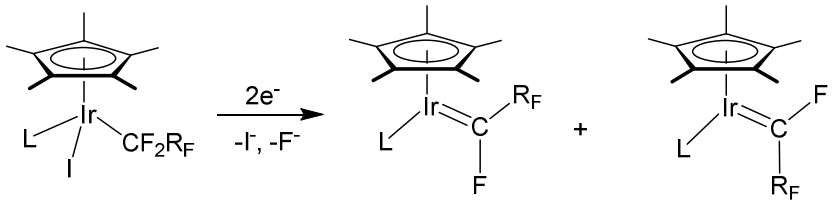

12 L = CO, R_F = CF_3
13 L = PMe_3, R_F = CF_3
14 L = CO, R_F = CF_2CF_3
15 L = PMe_3, R_F = CF_2CF_3
16 L = CO, R_F = C_6F_5
17 L = CO, R_F = F
18 L = PMe_3, R_F = F

In a typical procedure, Cp*(L)Ir(CF_2R_F)(I) was added to a THF suspension of magnesium graphite at room temperature, and subsequent hexane extraction yielded spectroscopically pure carbene complexes **12-16**. In general, the carbonyl compounds were found to be less air sensitive than the phosphine compounds and could even be purified on a neutral alumina column run in air at room temperature. The carbene compounds were characterized by X-ray crystallography as well as NMR and IR (ν_{CO}) spectroscopy and microanalysis.

ORTEP diagrams of **12b** (Figure 1), **15a** (Figure 2) and **16a** (Figure 3) are presented below. The X-ray crystal structures clearly confirm formation of the carbene ligands. Except for the perfluorobenzylidene complex **16a**, the crystallographically characterized isomer was the major isomer formed in the synthesis. Selected bond lengths and angles are shown in Table 1, along with a comparison of the crystallographic structures with those determined by Density Functional Theory (DFT) using the B3LYP functional[40-44] with the Grimme D3 dispersion correction,[45, 46] and the LACV3P**++ basis set.[47-50] DFT

calculated structures for those isomers not characterized crystallographically are also included in Table 1. Structures of compounds **13a**,[28] **14b**[37] **17**[37] and **18**[28] have been previously reported, but comparative data are included with those for **12b, 15a** and **16a**.

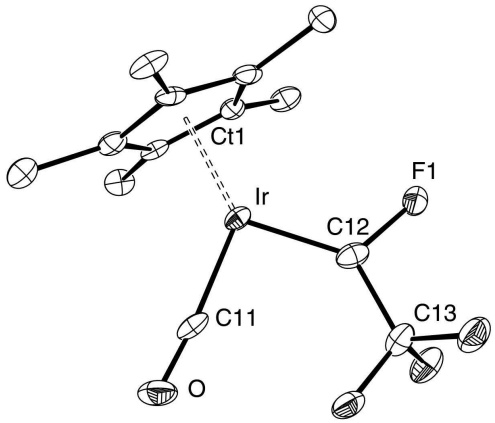

Figure 1. ORTEP diagram of the non-hydrogen atoms of isomer **12b**, showing a partial atom-labeling scheme. Thermal ellipsoids are shown at the 30% level. Two independent molecules crystallized in the asymmetric unit. Selected bond distances (Å) and angles (º): Ir-C12, 1.875(10), 1.852(10); C12-F1, 1.383(12), 1.385(11); C12-C13, 1.495(14), 1.529(14); Ir-C11, 1.843(11), 1.860(10); C11-O1, 1.159(12), 1.142(11); Ir-Ct, 1.880(9), 1.886(10); C11-Ir-C12, 95.0(4), 95.4(4); F1-C12-Ir, 121.1(7), 122.7(7); F1-C12-C13, 103.2(8), 102.1(8); C13-C12-Ir, 135.7(8), 135.2(8); Ct-Ir-C11, 131.24(4), 131.11(4); Ct-Ir-C12, 133.73(4), 133.50(4).

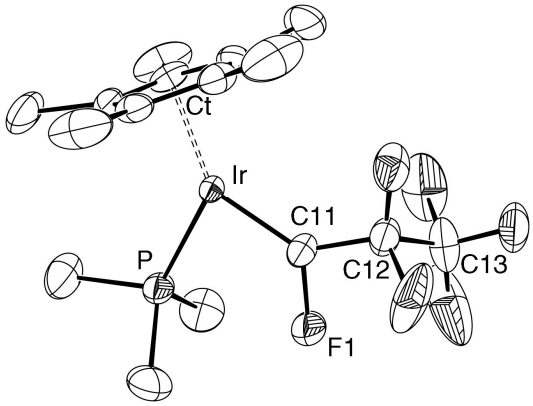

Figure 2. ORTEP diagram of the non-hydrogen atoms of the isomer **15a**, showing a partial atom-labeling scheme. Thermal ellipsoids are shown at the 30% level. Selected bond distances (Å) and angles (º): Ir-C11, 1.864(6); Ir-P, 2.2445(18); F1-C11, 1.441(7); C11-C12, 1.455(9); Ir-Ct 1.916(6); Ct-Ir-C11, 142.27(3); Ct-Ir-P, 132.02(19); F1-C11-Ir, 126.9(4); C11-Ir-P, 85.6(2).

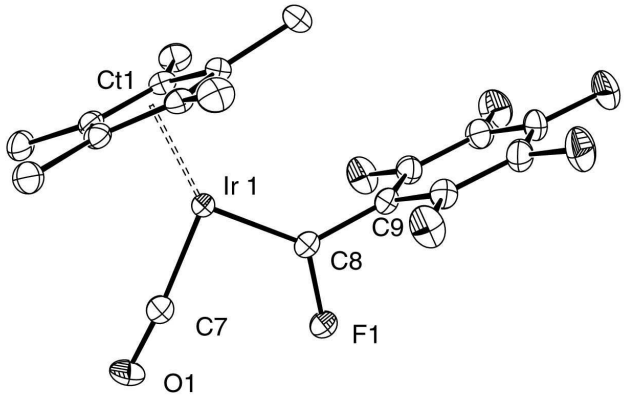

Figure 3. ORTEP diagram of the non-hydrogen atoms of isomer **16a**, showing a partial atom-labeling scheme. The molecule lies on a crystallographic mirror plane. Thermal ellipsoids are shown at the 30% level. Selected bond distances (Å) and angles (º): Ir-C8, 1.858(4); Ir-C7, 1.850(5); Ir-Ct 1.903(4); F1-C8, 1.390(5); C8-C9, 1.503(6); C7-Ir-C8 90.3(2); F1-C8-Ir 124.3(3); C9-C8-Ir, 130.4(3); Ct-Ir-C7, 130.51(18); Ct-Ir-C8, 139.20(17).

Table 1. Comparison of selected bond lengths and angles in the crystal structures of perfluoroalkyl carbene complexes and DFT/B3LYP-D3/LACV3P**++ calculated structures (**boldface**). Two independent molecules of **12b** crystallized in the unit cell, and data for both compounds are shown.

	R_F	L	Ir=C(Å)	L-Ir-C(º)	F-αC-R_F(º)	Ct-Ir-L(º)	Ct-Ir-αC(º)
17	F	CO	1.855(13) **1.879**	91.7(5) **91.4**	103.5(10) **105.0**	133.3(4) **133.9**	135.1(4) **134.7**
18	F	PMe_3	1.854(11) **1.859**	89.1(4) **90.0**	104.3(9) **103.0**	133.5(4) **133.8**	137.4(4) **136.1**
12a	CF_3	CO	**1.884**	**90.5**	**106.1**	**130.0**	**139.6**

12b	CF_3	CO	1.875(10) 1.852(10) **1.880**	95.0(4) 95.4(4) **95.4**	103.2(8) 102.1(8) **104.6**	131.24(4) 131.11(4) **131.2**	133.73(4) 133.50(4) **133.4**
13a	CF_3	PMe_3	1.845(10 **1.872**	88.1(4) **88.8**	99.2(9) **104.7**	139.9(4) **132.2**	132.0(4) **139.0**
13b	CF_3	PMe_3	**1.871**	**96.6**	**102.7**	**131.4**	**131.8**
14a	C_2F_5	CO	**1.885**	**90.0**	**105.7**	**129.1**	**140.9**
14b	C_2F_5	CO	1.880(10) **1.880**	95.2(4) **95.1**	104.2(8) **106.0**	129.42(4) **131.7**	135.39(4) **133.09**
15a	C_2F_5	PMe_3	1.864(6) **1.873**	85.6(2) **88.2**	99.2(5) **103.3**	132.02(19) **131.1**	142.27(3) **140.6**
15b	C_2F_5	PMe_3	**1.870**	**96.7**	**102.4**	**131.8**	**131.5**
16a	C_6F_5	CO	1.858(4) **1.880**	90.3(2) **91.5**	105.4(3) **108.1**	130.51(18) **133.5**	139.20(17) **135.1**
16b	C_6F_5	CO	**1.875**	**91.3**	**108.5**	**132.1**	**136.6**

The DFT calculated structures show excellent agreement with the metrics determined crystallographically, and for the most part are within the ESDs for the crystallographic values, boosting confidence in the calculated DFT metrics for the non-crystallographically characterized isomers. All the complexes show Ir=C distances of between 1.8-1.9 Å with no significant differences for CO or PMe_3 analogues. These are significantly less than a typical Ir-R_F distances of ~2.1 Å for the starting perfluoroalkyl compounds[51] and are consistent with double bond character between the iridium and the α-carbon. In general the L-Ir-C_α angles are in the range of 85-95° while the two angles between the ligated atoms of the carbene or L and the Cp* centroids (Ct) are significantly larger, in the 130-140° range. For the Ir=CF_2 complexes **17** and **18** these inter-ligand angles are almost independent of whether the ancillary ligand is CO or PMe_3. Introduction of a CF_3 group on the carbene ligand in the isomers of compound **12** results in opening of the OC-Ir-C when CF_3 is cis to CO (**12b)** and corresponding contracting of the Ct-Ir-C angle, illustrating some steric interaction between CO and the cis-CF_3 group. Nevertheless the Z-isomer **12b** is the major one observed experimentally in solution (see below), and is

predicted by DFT to have a free energy 3.0 kcal/mol lower than **12a**. Replacement of CO by PMe_3 to give perfluoroethylidene compounds **13** reverses this order of stability and the E-isomer **13a** is predicted to be 3.0 kcal/mol lower than **13b**. The opening of the Me_3P-Ir-C angle and contraction of the Ct-Ir-C angle between isomers **13a** and **13b** are both more pronounced than for the CO analogues **12**. Thus the isomer energetics appear to be determined predominantly by steric effects between the CF_3 group and the ancillary ligand at 90°. Likewise the perfluoropropylidene complexes show a preference for the Z-isomer when L=CO (**14b** is 1.6 kcal/mol more stable than **14a**) and the E-isomer when L=PMe_3 (**15a** is 3.0 kcal/mol more stable than **15b**). Similar angle variations are observed. For the perfluorobenzylidene complexes **16** the free energy difference is less pronounced, with the Z-isomer **16a** being only 0.6 kcal/mol lower in energy than its E-analogue; notably in both isomers the pentafluorophenyl ring is essentially perpendicular to the L-Ir-C_α plane, with less two-dimensional steric demand than a three dimensional perfluoroalkyl group.

The NMR data are also characteristic for perfluoroalkylcarbene ligands. Typical features include very low field chemical shifts for the α-carbon and fluorine[7, 10, 29, 52] and a large $^1J_{CF}$ (~300-350 Hz) coupling.[28, 29] The α-fluorine also couples with the other fluorines in the ligand chain. In the phosphine compounds an additional three bond coupling is observed between the α-fluorine and the phosphorus, which is larger in the isomers in which phosphorus and the α-fluorine are cis, as observed previously for fluoroaryl complexes.[53] In the minor isomer of **16** a long range coupling is observed between the carbene fluorine and the *p*-fluorine of the phenyl ring ($^6J_{FF}$ = 5 Hz); this coupling has previously been observed in several fluorinated styrene compounds[54] as well as in the previously reported perfluorobenzylidene compound, Cp*(PMe_3)Ir=CFC_6F_5.[28]

Finally, the formal reduction of the metal from iridium Ir^{III} to Ir^{I} is indicated by a decrease (~30 cm^{-1}) in the carbonyl stretching frequency. For example, in reducing Cp*(CO)Ir(I)($CF_2CF_2CF_3$) to **14** the value of ν_{CO} decreases from 2050 cm^{-1} (hexanes)[51] to 2011 cm^{-1} (hexanes).[37]

Interconversion of E/Z Geometric Isomers.

Under ambient light conditions the carbene complexes are formed in this reductive procedure as variable mixtures of E/Z diastereomers. The geometries in solution were determined by $^{19}F\{^{1}H\}$ Heteronuclear Overhauser (HOESY) NMR experiments, analogous to those we have used previously to determine configurations and conformations in fluorinated organometallic compounds of this type.[55] For example, in the carbonyl complexes **12**, **14** and **16** the major Z-isomers showed a strong cross-peak between the α-fluorine and the Cp* proton resonance, indicating a <5Å average distance between these two groups, while the minor isomer showed a cross-peak between Cp* and fluorines in the R_F group.<Bourgeois, 2006 #8420> *As noted above it was incorrectly reported earlier that the major isomer of **12** adopted the E configuration*.[37] For the PMe_3 analogues **13** and **15** the major E-isomers showed a cross-peak between the α-fluorine and the PMe_3 and the minor isomers a cross-peak between Cp* and the α-fluorine. As discussed above, this can be rationalized on steric grounds bearing in mind the approximately 90° relationship between L and the carbene ligand. In every case except that of the perfluorobenzylidene complex **16** the major isomer was the one that crystallized from solution, allowing samples containing individual E- and Z-isomers to be obtained.

On stirring a solution of the pure Z-isomers of carbonyl complexes **12a** and **14a** under ambient light the E isomer slowly increased in concentration; similar treatment of the E-isomers of PMe_3 complexes **13b** and **15b** resulted in slow increase in concentration of the corresponding Z-isomers. Eventually in each case an apparent photostationary state[56] was reached. In the dark, each mixture returned even more slowly to its equilibrium isomer ratio; this process was accelerated by heating. Figure 4 illustrates the isomerization of **14a** and Scheme 4 shows the ratios of E- and Z-isomers in the photostationary state, and after thermal equilibration. This constitutes a rare example of photoisomerization of an carbene complex.[57] No attempts were made to determine any frequency dependence or other quantitative aspects of this ambient light photoisomerization. It simply provided a convenient way in which non-equilibrium mixtures of diastereomers could be obtained, and their thermal return to equilibrium monitored kinetically.

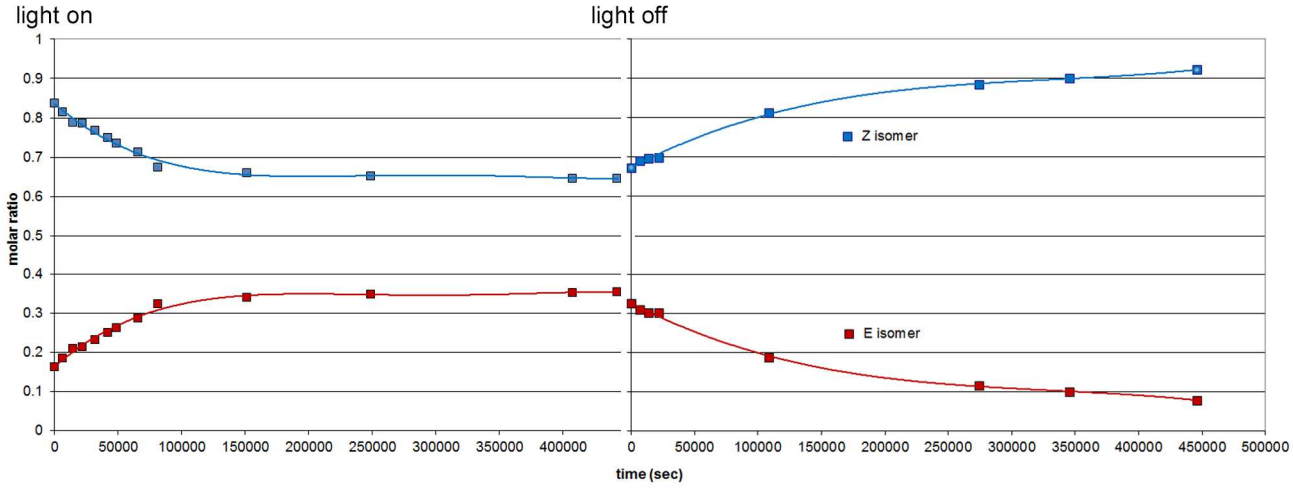

Figure 4. Time course of the interconversion of the Z- and E-isomers of complex **14** on exposure to ambient light (C_6H_6 solution, 20°C), followed by removal of the light source.

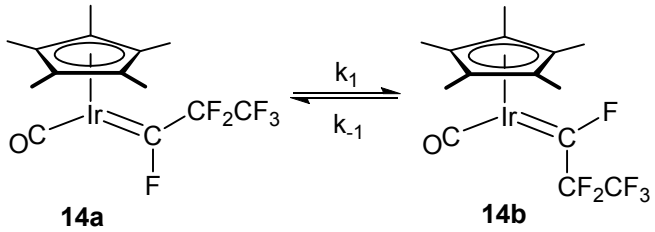

14a **14b**

1	photostationary ratio	2
1	thermal ratio	12

Scheme 4

Concentrations of isomers were measured by ^{19}F NMR integration over time for the thermal return to equilibrium at four different temperatures (30, 40, 47, and 55ºC). The difference between the initial concentration, $[A]_0$ and the concentration at time t is X and at equilibrium X = X_e. A plot of $\ln(X_e-X)$ versus t gave a straight line with slope equal to $-(k_1+k_{-1})$. Knowledge of K_{eq} allows k_1 and k_{-1} to be determined.[58] An Eyring plot of ln(k/T) versus 1/T gives the thermodynamic parameters for thermal isomerization by rotation about the Ir=C bond as $\Delta H^{\ddagger}$ = 19 kcal/mol, $\Delta S^{\ddagger}$ = -25 cal/mol, and $\Delta G^{\ddagger}_{298}$ = 25 kcal/mol. The value for the free energy barrier for this rotation calculated by DFT (B3LYP/LACV3P**++) is 27 kcal/mol, in excellent agreement with experiment.

Recognition of the role of ambient light in the E/Z isomerization of these perfluorocarbene complexes, led to reductive synthesis *in the dark* which afforded formation of a single E-stereoisomer

for PMe_3 compounds and Z-stereoisomer for CO compounds; only on workup did slow photoisomerization commence. Clearly the favored isomer in the synthesis is the thermodynamically favored one. This dark synthesis coupled with the slow approach to, and return from, the non-equilibrium photostationary state provided us with the capability of obtaining different ratios of the E/Z isomers that changed very slowly with time.

Addition Reactions of Perfluoroalkylcarbene Complexes with HCl

Addition of HCl in toluene to a toluene solution of the Z-perfluoroalkylcarbene complexes **12b**, **14b** or **16b** at low temperature resulted in rapid addition of HCl across the double bond to yield single diastereomers of **19b**, **21b** and **23b** respectively, which were configurationally stable in toluene solution, and each of which was characterized crystallographically. ORTEP diagrams are presented in Figures 5-7 and clearly define the regiochemistry and stereochemistry of addition. The protons on the α-carbons were not located crystallographically, but their presence and the stereochemistry at the α-carbon atoms are clear.

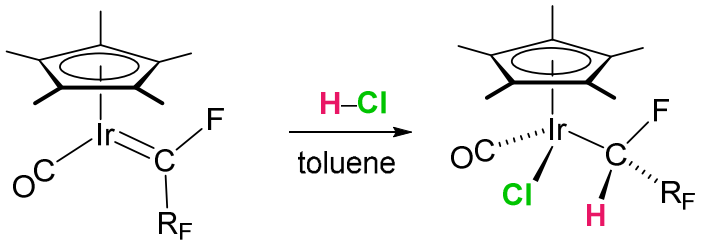

12b $R_F = CF_3$
14b $R_F = CF_2CF_3$
16b $R_F = CF_2C_6F_5$

19b $R_F = CF_3$
21b $R_F = CF_2CF_3$
23b $R_F = CF_2C_6F_5$

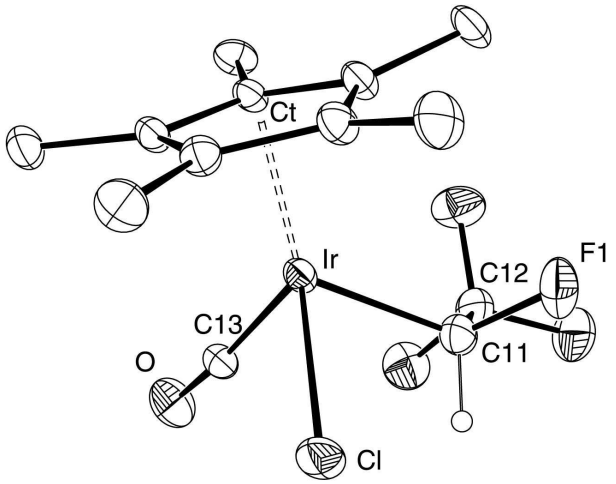

Figure 5. ORTEP diagram of the non-hydrogen atoms of **19b**, showing a partial atom-labeling scheme. The hydrogen attached to C11 is shown. Thermal ellipsoids are shown at the 30% level. Selected bond distances (Å) and angles (º): Ir-C11, 2.091(5); C11-F1, 1.397(6); Ir-Cl, 2.3979(13); Ir(1)-C(13), 1.882(5); C13-O, 1.121(6); C(13)-Ir(1)-Cl(1) 92.64(15); C(11)-Ir(1)-Cl(1), 83.89(14); C(13)-Ir(1)-C(11) 90.6(2); Ir-C11-C12, 118.6(3); F1-C11-C12, 105.4(4).

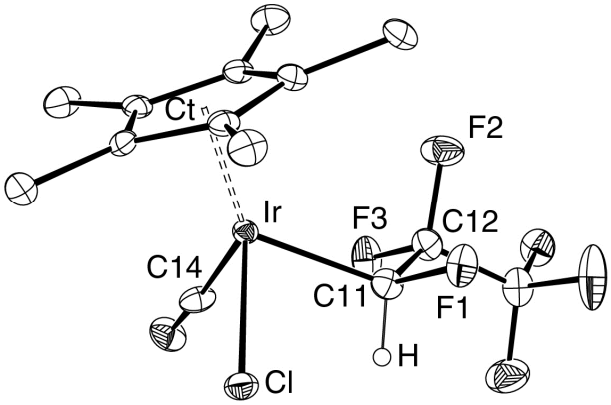

Figure 6. ORTEP diagram of the non-hydrogen atoms of **21b**, showing a partial atom-labeling scheme. The hydrogen attached to C11 is shown. Thermal ellipsoids are shown at the 30% level. Selected bond lengths (Å) and angles (°): Ir-C14, 1.884(7); Ir-Cl, 2.3949(13); Ir-C11, 2.093(6); C11-C12, 1.486(8);

C11-F1, 1.4131(6); C14-Ir-C11, 89.2(3); C14-Ir-Cl, 93.07(18); Cl-Ir-C11, 82.87(18); Ir-C11-C12, 117.9(4); F1-C11-C12, 105.3(5).

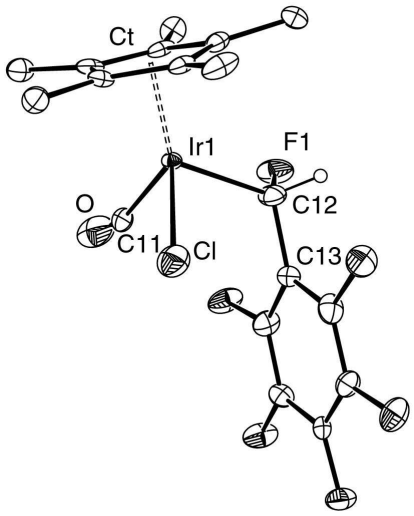

Figure 7. ORTEP diagram of the non-hydrogen atoms of **23b**, showing a partial atom-labeling scheme. The hydrogen attached to C12 is shown. Thermal ellipsoids are shown at the 30% level. Selected bond lengths (Å) and angles (°): Ir-C11, 2.038(10); Ir-Cl, 2.367(2); Ir-C12, 2.086(9); C12-C13, 1.512(10); C12-F1, 1.452(11); C11-Ir-C12, 88.7(4); C12-Ir-Cl, 91.2(3); F1-C12-C13, 107.5(6); F1-C12-Ir 109.3(6).

Each structure shows that addition of HCl occurred regiospecifically, with the electrophilic $H^{\delta+}$ adding to C and $Cl^{\delta-}$ to Ir. It is also clear that each structure resulted from an exclusive cis-addition of HCl to the original Z-isomer of the respective perfluorocarbene complex. As an extra check that the crystallographically determined structure was not that of a rogue crystal arising from a tiny amount of another diastereomer or regio-isomer present in small enough amounts so as to be invisible by NMR, each crystallographic determination was followed by dissolution of the specific crystal on which the diffraction experiment was performed, and determination of its NMR spectra. In all cases the spectra of the dissolved crystal matched those of the observed product, confirming the correlation between the crystallographic structure and the solution data. In structures **19b** and **21b** the fluoroalkyl ligand conformation is that in which the R_F group situates itself in the region of space between Cp* and CO,

while the F sits between Cp* and Cl and the H occupies the smallest space, between CO and Cl (Figure 4).

The NMR spectra confirm addition of the hydrogen to the carbene carbons; the H resonates at low field, between δ 6.5 and 7 ppm, and shows large coupling with the geminal fluorine ($^2J_{HF}$ ~ 47 Hz). This proton also couples with the fluorines on the β-carbon. The α-fluorine, which resonates far downfield in the carbene compound (*vide supra*) moves upfield by almost 200 ppm in the alkyl product to around δ –190 ppm and show a large coupling to the geminal proton as well as the other fluorines in the molecule. The perfluorobenzyl product **23b** again shows long range coupling ($^6J_{FF}$ = 2 Hz).

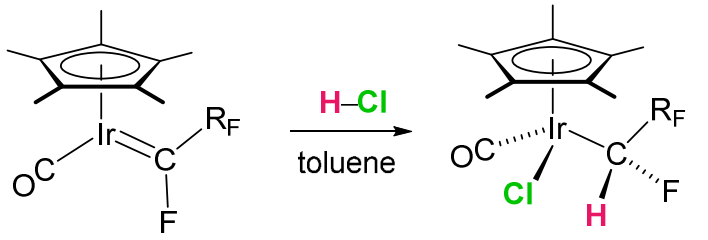

12a $R_F = CF_3$
14a $R_F = CF_2CF_3$
16a $R_F = C_6F_5$

19a $R_F = CF_3$
21a $R_F = CF_2CF_3$
23a $R_F = C_6F_5$

Various isomeric ratio of perfluorocarbene precursors were obtained by varying their exposure to light. Addition of HCl to an X:1 ratio of **12b:12a** (X = 2, 6, 11) gave X:1 ratios of diastereomeric products **19b:19a**. Likewise X:1 ratios of **14b:14a** (X = 3, 20) gave identical X:1 ratios of **21b:21a**, and a 5:1 ratio of **16b:16a** gave a 5:1 ratio of **23b:23a**. In all cases the individual product ratios did not change on heating in toluene, indicative of configurational stability. Clearly, if pure **12b** gives only pure **19b**, then isomer **12a** must give only **19a**. The addition is both regio- and stereospecific in all three cases.

Identical regiochemical and stereochemical conclusions result from reactions of the PMe_3 analogues with HCl. Reaction of pure E isomer **13a** yielded a single diastereomer of **20a** while a 4:1 mixture of **15a:15b** yielded a 4:1 ratio of **22a:22b**. The major diastereomers **20a** and **22a** have been previously reported and fully characterized.[33]

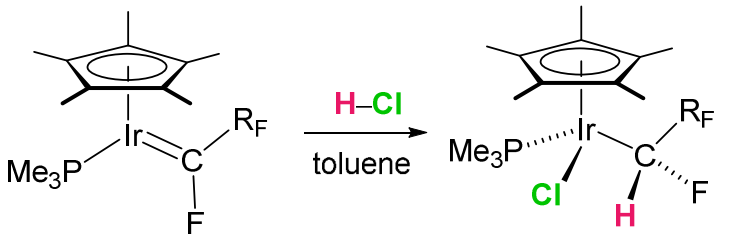

13a $R_F = CF_3$
15a $R_F = CF_2CF_3$

20a $R_F = CF_3$
22a $R_F = CF_2CF_3$

The previously reported[59] bis(trifluoromethyl)carbene complex **24** also reacted with HCl to afford addition product **25** with identical regiochemistry.

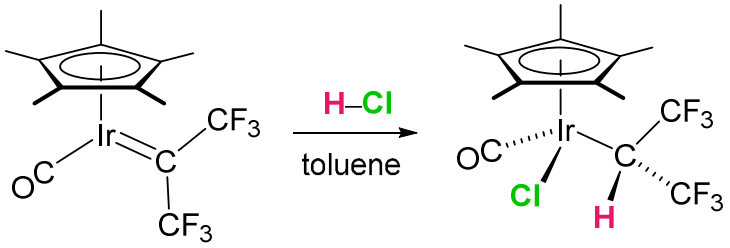

24 **25**

The observed regiochemistry of HCl addition to the perfluorocarbene complexes **12a-16a** and **24** parallels that observed previously in addition of HI to the corresponding $Cp^*(PMe_3)Ir{=}CF_2$ complex **18** to give **26**.[28] In that study it was shown that addition of triflic acid to **18** at low temperatures resulted in cation **27**, in which the added proton resided on Ir, while protonation of the $CF(CF_3)$ analogue **13** afforded **28** in which the proton was bound to C; whether or not triflate was bound to Ir could not be determined.

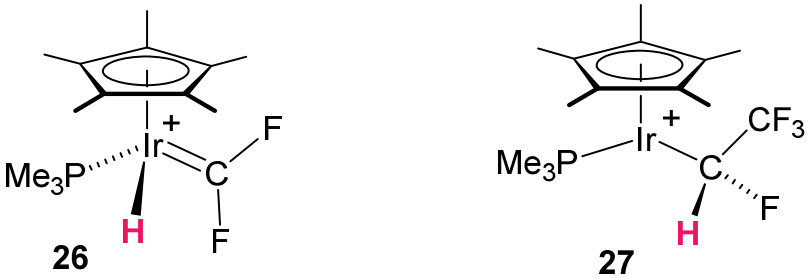

26 **27**

Taken together, these results illustrate that, regardless of whether the free perfluorocarbene ligand is a ground state singlet or a triplet, the experimentally observed products of HCl addition are invariably those formed by electrophilic $H^{\delta+}$ adding to C and $Cl^{\delta-}$ to Ir. However, the observation of **26**

and observations from our group, [31-34] and others, [21, 22] [10, 25, 26] that H (and other groups) can migrate from their original locus on a metal to the perfluorocarbene carbon in the presence of a coordinating anion, in some cases with complete preservation of stereochemistry at C and at Ir, calls into question whether the HCl adducts formed here are those resulting from a kinetic controlled addition, or whether an initial protonation at Ir, followed by H-migration to C is a viable pathway.

DFT Studies of the Addition of HCl.

In the absence of further experimental approaches, these pathways have been examined using DFT, for HCl addition to the model compounds $Cp(PH_3)Ir{=}CF_2$, E-$Cp(PH_3)Ir{=}CFCF_3$, and $Cp(PH_3)Ir{=}C(CF_3)_2$. Since all the observed chemistry occurs at low temperature in a non-polar and poor donor solvent (toluene) a solvent model was not included. For each pre-optimized carbene ligand system starting structures were generated by placing a pre-optimized HCl at several initial distances (d) and angles (θ) from the Ir=C double bond, as shown for $Cp(PH_3)Ir{=}CF_2$ in Figure 8, thereby providing some reasonable constraints to the complex hypersurface. Saddle points having a single imaginary frequency and linking each of these starting structures and each appropriate regio-isomeric product were sought. For each regiochemistry the same transition states were found regardless of the starting angle (θ) between the reactants. Free energy profiles for all three systems are shown in Figure 9, and calculated geometries for starting materials, transition states, and products are provided in Figure 10. Table 2 presents Natural Population Analysis (NPA) charges on selected atoms in starting materials and transition states. Full structural and calculation details are provided as Supplementary Information.

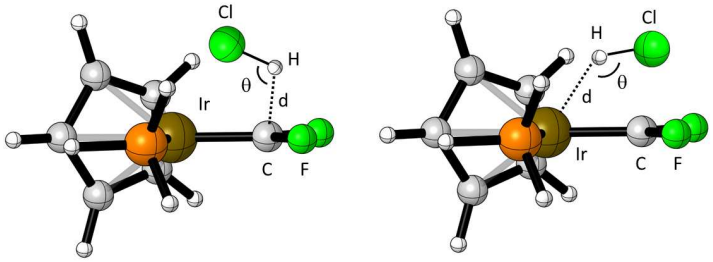

Figure 8. Starting structures for location of transition states for the two regiochemistries for HCl $Cp(PH_3)Ir{=}CF_2$; (d = 1-2Å in increments of 0.1Å) from Ir or C to the $H^{\delta+}$ electrophile; θ = 90-180° in increments of 10°; with an Ir=C/H-Cl dihedral angle of 0°). Analogous constraints were applied to the two other carbene systems studied.

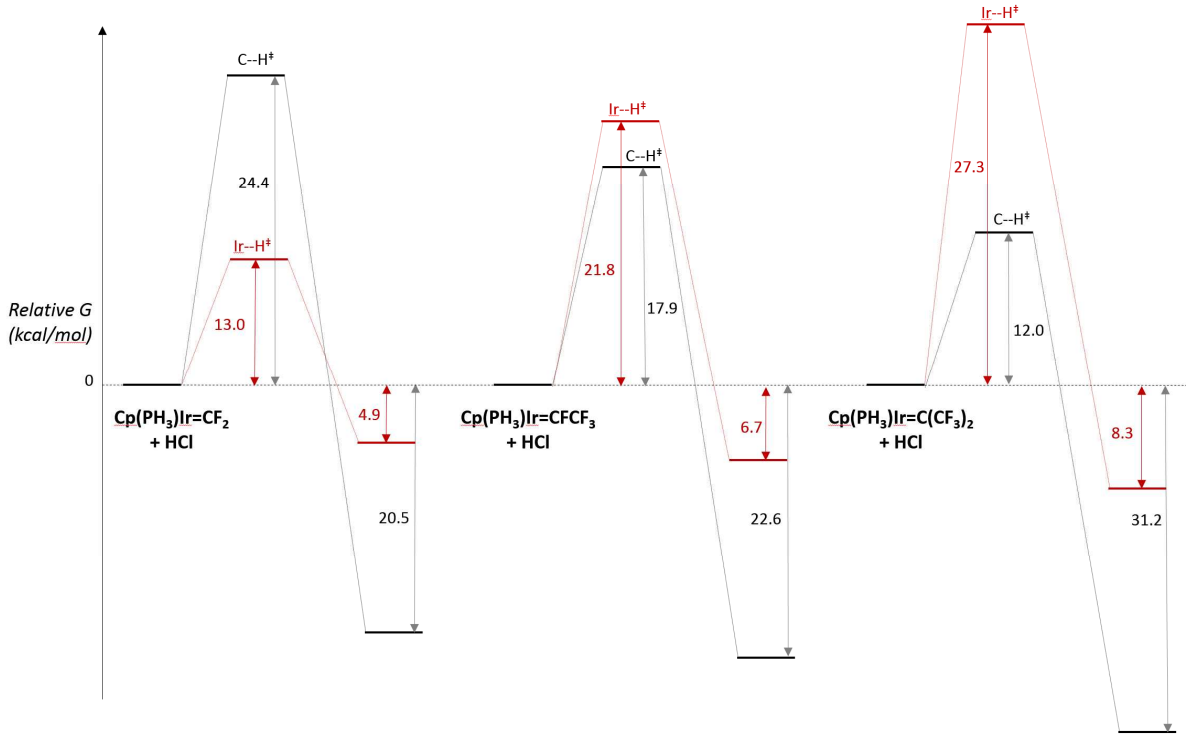

Figure 9. DFT calculated (B3LYP-D3/LACV3P**++) free energy profiles for the two regiochemical modes of addition of HCl to $Cp(PH_3)Ir{=}CF_2$, E-$Cp(PH_3)Ir{=}CFCF_3$, and $Cp(PH_3)Ir{=}C(CF_3)_2$ via the transition states shown in Figure 10. Pathways involving electrophilic addition of $H^{\delta+}$ to C are linked by grey arrows; pathways involving electrophilic addition of $H^{\delta+}$ to Ir are linked by red arrows.

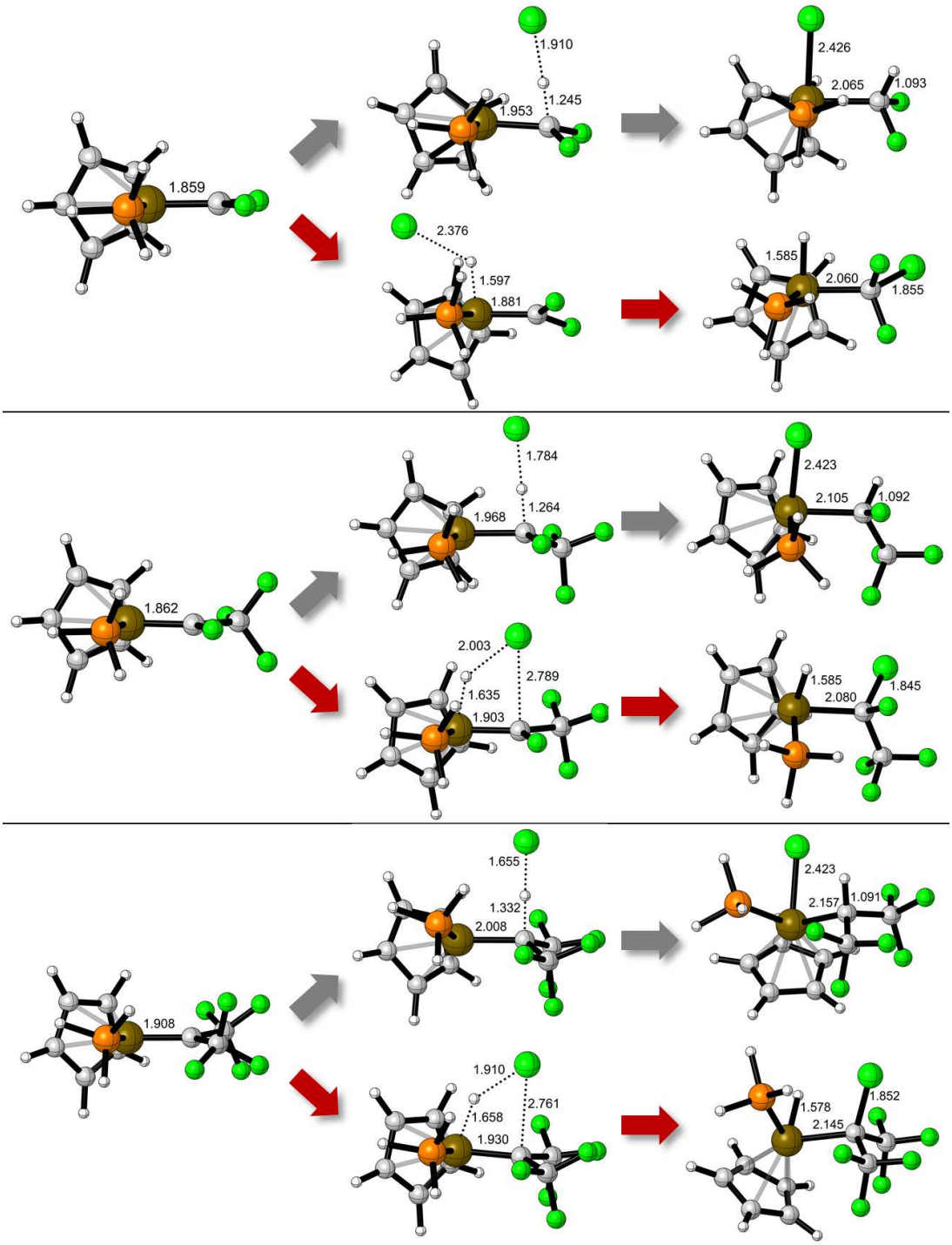

Figure 10. DFT calculated (B3LYP-D3/LACV3P**++) structures for starting materials, transition states, and products for the two regiochemical modes of addition of HCl to $Cp(PH_3)Ir{=}CF_2$, E-$Cp(PH_3)Ir{=}CFCF_3$, and $Cp(PH_3)Ir{=}C(CF_3)_2$. Pathways involving electrophilic addition of $H^{\delta+}$ to C are linked by grey arrows; pathways involving electrophilic addition of $H^{\delta+}$ to Ir are linked by red arrows.

Table 3. Natural Population Analysis (NPA) charges in starting materials and transition states for HCl addition reactions.

Compound	Ir	C	H	Cl	P
H-Cl	-	-	+0.25	-0.25	-
$Cp(PH_3)Ir=CF_2$	+0.07	+0.59	-	-	+0.38
C-H TS	+0.29	+0.41	+0.23	-0.70	+0.37
Ir-H TS	+0.15	+0.70	+0.14	-0.82	+0.47
$Cp(PH_3)Ir=CFCF_3$	+0.24	+0.14	-	-	+0.39
C-H TS	+0.32	-0.08	+0.25	-0.63	+0.37
Ir-H TS	+0.14	+0.36	+0.16	-0.63	+0.43
$Cp(PH_3)Ir=C(CF_3)_2$	+0.25	-0.41	-	-	+0.38
C-H TS	+0.37	-0.62	+0.27	-0.54	+0.37
Ir-H TS	+0.18	-0.15	+0.18	-0.54	+0.44

It is clear from the reaction energetics that in all three systems the product observed experimentally, arising from addition of H to C and Cl to Ir, is calculated to be strongly preferred thermodynamically over the other regioisomer. However there are significant differences in the kinetically preferred pathways. For the $Ir=CF_2$ system, the transition state leading to the Ir-H product lies well below that for the C-H transition state. Successive introduction of CF_3 groups on the carbene leads to progressive stabilization of the C-H transition state and destabilization of the Ir-H transition state, so that for the $Ir=CFCF_3$ and $Ir=C(CF_3)_2$ systems the C-H transition state is preferred. Clearly the observed regiochemistry for the CF_3 substituted carbenes is both kinetically and thermodynamically preferred. So why is a different pathway kinetically favorable in the $Ir=CF_2$ system?

Comparison of the NPA charges in the Ir=C functional group in the starting carbene complexes illustrates the dramatic diminution of positive charge at carbon on changing from $CF_2 \rightarrow CFCF_3$. Introduction of a second CF_3 group results in a negative charge on carbon in the $C(CF_3)_2$ starting material. This is consistent with the idea that π-donor F-substituents help stabilize adjacent positive carbon while exclusively acceptor (σ and π) CF_3 substituents better stabilize adjacent negative charge,

and also with the resonance structure arguments presented in the introduction. In all three cases the calculated transition states for reaction of the carbon terminus of the Ir=C functional group with the electrophilic $H^{\delta+}$ of HCl involves an almost linear C--H--Cl angle, with progressively longer C--H and shorter H--Cl distances on going from $CF_2 \rightarrow CFCF_3 \rightarrow C(CF_3)_2$. There is also considerable lengthening of the Ir-C bond and pyramidalization at C, consistent with the π-electrons of the Ir=C bond being used to bind to HCl . Compared to free HCl, the NPA charges on H in the C-H transition states remain essentially unchanged, while the charge on Cl becomes substantially more negative. In the Ir-H transition states the Ir--H--Cl angle is significantly more bent, the H is less positive than free HCl while the charges on Cl remain essentially identical to those in the CH transition states. In addition there is considerably less lengthening of the Ir-C bond and very little pyramidalization at C, consistent with interaction of HCl with a non-bonding Ir d-electron pair. In the C-H transition states there is an increase in negative charge (or decrease in positive charge) at C and an increase in positive charge at Ir; the positive charge at P remain constant. In contrast, the Ir-H transition state NPAs reveal increased positive (or decreased negative charge) at C. By simple charge arguments, substituents best able to stabilize build-up of negative charge in the CH transition states should favor that pathway, and substituents best able to stabilize positive charge at C should favor the Ir-H pathway. The $Ir=CF_2$ and $C(CF_3)_2$ systems provide an unambiguous prediction, while the $Ir=CFCF_3$ system, with one of each type of substituent, is ambiguous.

We have been unable to locate computationally any additional intermediates or transition states corresponding to separate formation of the Ir-Cl (or C-Cl) bonds. We conclude that either these reactions are examples of extremely asynchronous concerted additions or that the barrier for formation of the eventual bond to Cl from any intermediate is extremely small. This is consistent with the stereochemical results described above for the $Ir=CFCF_3$ systems, in which preservation of stereochemical relationships between the C and Ir centers is preserved in the kinetically controlled products. The $Ir=CF_2$ system still remains frustratingly ambiguous and we cannot distinguish, experimentally or computationally, between: 1) a rapid, reversible addition of HCl to give an

unobserved, kinetically controlled, regioisomer, with a subsequent addition of opposite regiochemistry under thermodynamic control; or 2) a polar two step pathway involving protonation at Ir, followed by migration of H from Ir to C with rapid incorporation of chloride at the metal center. Experimental evidence for the latter pathway has been discussed (*vide supra*) but involves entry via a different reaction manifold and the conclusions do not necessarily transfer to the system studied here.

Conclusions.

Our most important conclusion is that the relative nucleophilicity or basicity of carbene ligands cannot necessarily be deduced by examination of the electronic structures of the starting materials, and certainly cannot be deduced by examination of product structure and regiochemistry, unless it is known that the observed product and its regiochemistry are the result of kinetic control. Here we have shown that the perfluorocarbene ligands $CF(CF_3)$ and $C(CF_3)_2$ *in these iridium complexes* are unequivocally basic (and probably nucleophilic) at carbon, but that the CF_2 ligand is less basic (or nucleophilic) than the iridium center to which it is bound and implicitly less basic than its perfluoroalkylcarbene relatives. We have not demonstrated electrophilic behavior for CF_2.

Experimental Section

All reactions were performed in oven-dried glassware, using standard Schlenk techniques, under an atmosphere of nitrogen which had been deoxygenated over BASF catalyst and dried over molecular sieves or in a Braun drybox. Solvents were deoxygenated and dried over activated alumina under nitrogen.[60] NMR spectra were recorded on a Varian Unity Plus 300 or 500 FT spectrometer at 21°C. ^{1}H NMR spectra were reference to the protio impurity in the solvent: C_6D_6 (7.16 ppm). ^{19}F NMR spectra were referenced to external $CFCl_3$ (0.00 ppm). ^{31}P NMR spectra were referenced to external 85% H_3PO_4. Coupling constants are reported in Hertz and are absolute values. IR spectra were recorded on a Perkin-Elmer FTIR 1600 Series spectrophotometer. Elemental analyses were performed by Schwartzkopf (Woodside, NY) and X-ray crystallographic analyses at the University of California, San

Diego. HCl/toluene was prepared by bubbling HCl into dry, deoxygenated toluene and determining the concentration by titration with standard NaOH. Potassium graphite and magnesium graphite were prepared using literature procedures.[61, 62] Compounds Cp*(CO)Ir(CF_2CF_3)(I), Cp*(PMe_3)Ir(CF_2CF_3)(I), Cp*(CO)Ir($CF_2CF_2CF_3$)(I), Cp*(PMe_3)Ir($CF_2CF_2CF_3$)(I), and Cp*(CO)Ir($CF_2C_6F_5$)(I),[51] Cp*(CO)Ir=$CFCF_3$ **12**,[37] Cp*(PMe_3)Ir=$CFCF_3$ **13**,[28] Cp*(CO)Ir=$CFCF_2CF_3$ **14**[37] and Cp*(CO)Ir=$C(CF_3)_2$ **24**[59] were prepared as previously described. More detailed experimental procedures for **12-14** are included here.

Cp*(CO)Ir=$CFCF_3$ 12

A Schlenk flask was charged with potassium graphite (0.4485 g, 3.318 mmol) and magnesium chloride (0.1582 g, 1.66 mmol) and THF (3 mL) added. The mixture was refluxed for 30 min. Cp*(CO)Ir(CF_2CF_3)(I) (0.100 g, 0.166 mmol) was added as a solution in THF (3 mL) at room temperature and the suspension allowed to stir at room temperature (1 hour). The solvent was removed, the product extracted into hexanes, and the solvent removed to give a yellow solid (55 mg, 73%), found to be a mixture of isomers: major-Z (**12b**):minor-E (**12a**): 10:1. Anal Calcd for $C_{13}H_{15}F_4IrO$ (455.48): C, 34.37; H, 3.45. Found: C, 34.28; H, 3.32. IR (hexanes) ν_{CO} = 2010 cm^{-1}. **12b**: ^{1}H NMR (500 MHz, C_6D_6, 21°C) δ 1.69 (s, C_5Me_5). ^{19}F NMR (470 MHz, C_6D_6, 21°C) δ -73.2 (d, $^3J_{FF}$= 12 Hz, 3F), -0.1 (q, $^3J_{FF}$= 12 Hz, 1F). ^{13}C NMR (125 Hz, C_6D_6, 21°C) δ 9.4(s, 5C, C_5**Me$_5$**), 98.6(s, 5C, **C$_5$**Me_5), 129.1(qd, $^1J_{CF}$= 278 Hz, $^2J_{CF}$= 42 Hz, 1C, CF_3), 177.7 (qd, $^4J_{CF}$= 3 Hz, $^3J_{CF}$= 2 Hz, 1C, CO,), 208.5(dq, $^1J_{CF}$= 354 Hz, $^2J_{CF}$= 38 Hz, 1C, CF). **12a**: ^{1}H NMR (500 MHz, C_6D_6, 21°C) δ1.68 (s, C_5Me_5). ^{19}F NMR (470 MHz, C_6D_6, 21°C) δ -72.93 (d, $^3J_{FF}$= 10 Hz, 3F), 9.58 (q, $^3J_{FF}$= 10 Hz, 1F). When the reaction was carried out and worked up in the dark, only isomer **12b** was produced.

Cp*(PMe_3)Ir=$CFCF_3$ 13

A Schlenk flask was charged with potassium graphite (84.4 mg, 0.624 mmol) and THF (5 mL) was added. $Cp^*_{(PMe3)Ir}(CF_2CF_3)(I)$ (40 g, 0.0628 mmol) was added as a solution in THF (3 mL) and the suspension was stirred at room temperature (1 hour). The solvent was removed, the product extracted into hexanes, filtered, and the solvent removed to give a yellow solid (23.6 mg, 75%), found to be a mixture of isomers: major-E (**13a**):minor-Z (**13b**): 11:1. **13a**: ^{1}H NMR (C_6D_6 500 MHz, 21^{o}C) δ 1.85 (m, C_5Me_5), 1.33(dd, $^2J_{PH}$ = 10 Hz, $^3J_{FH}$ = 1 Hz, PMe_3). ^{19}F NMR (C_6D_6, 470 MHz, 21^{o}C) δ -69.9 (d, $^3J_{FF}$ = 13 Hz, 3F), -14.2 (dq, $^3J_{PF}$ = 73 Hz, $^3J_{FF}$ = 13 Hz, 1F). ^{31}P{^{1}H}NMR (C_6D_6 202 MHz, 22^{o}C) δ -40.6 (dq, $^3J_{FP}$ = 73 Hz, $^4J_{FP}$ = 3 Hz, 1P, PMe_3). ^{13}C{^{1}H} NMR (125 MHz, C_6D_6, 21^{o}C) δ 10.8 (dq, J_{CP} = J_{CF} = 1 Hz, 5C, C_5**Me$_5$**), 21.3 (dd,$^1J_{CP}$ = 38 Hz, $^4J_{CF}$ = 2 Hz, 3C, PMe_3), 94.0 (dd, $^2J_{CP}$ = 3 Hz, $^3J_{CF}$ =1 Hz 5C, **C$_5$**Me_5), 130.0 (qdd, $^1J_{CF}$ = 279 Hz, $^2J_{CF}$ = 54 Hz, $^3J_{CP}$ = 1 Hz 1C, CF_3), 191.7 (dqd, $^1J_{CF}$ = 318 Hz, $^2J_{CF}$ = 38 Hz, $^2J_{CP}$ = 21 Hz, 1C, CF). **13b**: ^{1}H NMR (C_6D_6 500 MHz, 21^{o}C) δ 1.88 (d, $^4J_{PH}$ = 1.5 Hz C_5Me_5), 1.40(dq, $^2J_{PH}$ = 10 Hz, $^6J_{FH}$ = 1 Hz, PMe_3). ^{19}F NMR (C_6D_6, 470 MHz, 21^{o}C) δ -67.2 (dd, $^4J_{PF}$ = 4 Hz, $^3J_{FF}$ = 14 Hz, 3F), -1.6 (q, $^3J_{FF}$ = 14 Hz, 1F). ^{31}P{^{1}H}NMR (C_6D_6 121.42 MHz, 21^{o}C) δ -49.5 (q, $^4J_{FP}$ = 4 Hz, 1P, PMe_3). When the reaction was carried out and worked up in the dark, only isomer **13a** was produced.

Cp*(CO)Ir=CFCF$_2$CF$_3$ 14

A Schlenk flask was charged with potassium graphite (0.106 g, 0.784 mmol) and magnesium chloride (0.035 g, 0.368 mmol) and THF (5 mL) added. The mixture was refluxed for 30 min. $Cp^*(CO)Ir(CF_2CF_2CF_3)(I)$ (0.036 g, 0.055 mmol) was added at room temperature and the suspension allowed to stir at room temperature (1 hr 45 min). The solvent was removed, the product extracted into hexanes, and the solvent removed to give an analytically pure yellow solid, 0.018 g (64%). The NMR spectra showed formation of the two isomers of the carbene: major Z **14b:**minor E **14a** in a ratio of 4:1. Anal Calcd for $C_{14}H_{15}F_6IrO$ (505.46): C, 33.26; H, 2.99. Found: C, 33.23; H, 2.89. IR (hexanes) ν_{CO} = 2011 cm^{-1}. **14b**: ^{1}H NMR (C_6D_6, 500 MHz, 21°C) δ 1.70 (s, C_5Me_5). ^{19}F NMR (C_6D_6, 470 MHz, 21°C)

δ 12.8 (tq, $^3J_{FF}$ = 18 Hz, $^4J_{FF}$ = 9 Hz, 1F, CFC_2F_5), -81.9 (dt, $^4J_{FF}$ = 8Hz, $^3J_{FF}$ = 3 Hz, 3F, CF_3), -113.2 (dq, $^3J_{FF}$ = 18 Hz, $^3J_{FF}$ = 3 Hz, 2F, CF_2). **14a**: ^{1}H NMR (C_6D_6, 500 MHz, 21°C) δ 1.69 (s, C_5Me_5). ^{19}F NMR (C_6D_6, 470 MHz, 21°C) δ 4.3 (tq, $^3J_{FF}$ = 18 Hz, $^4J_{FF}$ = 8 Hz, 1F, CFC_2F_5), -82.0 (dt, $^4J_{FF}$ = 8 Hz, $^3J_{FF}$ = 3 Hz, 3F, CF_3) -113.7 (d, $^3J_{FF}$ = 19 Hz, 2F, CF_2). When the reaction was carried out and worked up in the dark, only isomer **14b** was produced.

Cp*(PMe$_3$)Ir=CFCF$_2$CF$_3$ 15

A Schlenk flask was charged with potassium graphite (0.090 g, 0.666 mmol) and THF (5 mL) added. To this suspension was added Cp*(PMe$_3$)Ir($CF_2CF_2CF_3$)(I) (0.0442 g, 0.0632 mmol) as a solid. The mixture was stirred at room temperature (4 h). The solvent was removed and the product extracted into hexanes, filtered and the solution evaporated. The product was recrystallized from hexanes at -78 ºC to yield a yellow solid 0.024 g (69%), found to be a mixture of isomers with a ratio: major E (**15a**):minor Z (**15b**): 3:1. Anal Calcd for $C_{16}H_{24}F_6IrP$ (455.48): C, 34.72; H, 4.37. Found: C, 32.67; H, 4.06. **15**[a]=: ^{1}H NMR (C_6D_6, 500 MHz, 21°C): 1.85 (s, 15H, Cp*), 1.31 (d, $^2J_{PH}$ = 10 Hz, 9H, PMe_3). ^{19}F NMR (C_6D_6, 470 MHz, 21°C): δ -11.6 (dtq, $^3J_{PF}$ = 79 Hz, $^3J_{FF}$ = 20 Hz, $^4J_{FF}$ = 11 Hz, 1F, CF), -81.6 (dt, $^4J_{FF}$ = 11 Hz, $^3J_{FF}$ = 4 Hz, 3F, CF_3), -109.2 (d, $^3J_{FF}$ = 20 Hz, 2F, CF_2). ^{31}P NMR (C_6D_6, 121 MHz, 21°C): δ -40.2 (d, $^3J_{PF}$ = 79 Hz, PMe_3. ^{13}C NMR (C_6D_6, 125 Hz, 21°C) δ 11.0 (dt, J_{CF} = 2 Hz, J_{CP} = 1 Hz, 5C, C_5**Me$_5$**), 21.4 (dd,$^1J_{CP}$ = 38 Hz, $^4J_{CF}$ =2 Hz, 3C, PMe_3), 94.3(dd, $^2J_{CP}$ = 3 Hz, $^3J_{CF}$ = 1 Hz 5C, **C$_5$**Me_5), 117.2 (qtdd, $^1J_{CF}$ = 289 Hz, $^2J_{CF}$ = 40 Hz, $^3J_{CF}$ = 5 Hz, $^4J_{CP}$ = 1 Hz 1C, CF_3), 117.7 (tdqd, $^1J_{CF}$ = 251 Hz, $^2J_{CF}$ = 55 Hz, $^2J_{CF}$ = 36 Hz, $^3J_{CP}$ = 1 Hz 1C, CF_2), 191.9 (dtd, $^1J_{CF}$ = 310 Hz, $^2J_{CF}$ = 37 Hz, $^2J_{CP}$ = 21 Hz,1C, CF). **15b**: ^{1}H NMR (C_6D_6, 500 MHz, 21°C): 1.87 (s, 15H, Cp*), 1.35 (d, J = 11 Hz, 9H, PMe_3). ^{19}F NMR (C_6D_6, 470 MHz, 21°C): δ -0.07 (dtq, $^3J_{PF}$ = 79, $^3J_{FF}$ = 20, $^4J_{FF}$ = 11 Hz, 1F, CF), -80.4 (dt, $^4J_{FF}$ = 13, $^3J_{FF}$ = 4 Hz, 3F, CF_3), -106.4 (d mult.$^3J_{FF}$ = 20 Hz, 2F, CF_2). When the reaction was carried out and worked up in the dark, only isomer **15a** was produced.

Cp*(CO)Ir=CFC$_6$F$_5$ 16

A Schlenk flask was charged with potassium graphite (0.100 g, 0.740 mmol) and THF (8 mL) was added. Solid Cp*(CO)Ir($CF_2C_6F_5$)(I) (0.0483 g, 0.0691 mmol) was added and the suspension allowed to stir at room temperature (1.5 hrs). The solvent was removed, the product extracted into hexanes and the solvent removed to yield a bright yellow film. Recrystallization from hexanes at -78°C yielded the product in an isomer ratio of 2.5:1. Yield 0.030 g, 78%. Anal. Calcd for $C_{18}H_{15}F_6IrO$ (553.5): C, 39.06; H, 2.73. Found: C, 39.21; H, 2.91. IR (hexanes) ν_{CO} = 1993 cm^{-1}. Major (Z isomer) ^{1}H NMR (C_6D_6, 500 MHz, 21°C): δ 1.87 (s, Cp*). ^{19}F NMR (C_6D_6, 470 MHz, 21°C): δ 44.5 (t, $^4J_{FF}$ = 11 Hz, 1F, CF), -142.5 (ddd, $^3J_{FF}$ = 24, $^4J_{FF}$ = 11, $^5J_{FF}$ = 8 Hz, 2F, *o*-CF_2), -155.3 (t, $^3J_{FF}$ = 21 Hz, 1F, *p*-CF), -163.2 (ddd, ^5J = 24, $^3J_{FF}$ = 21, ^3J = 8 Hz, 2F, *m*-CF_2). Minor: (E isomer) ^{1}H NMR (C_6D_6, 500 MHz, 21°C): δ 1.48 (s, Cp*). ^{19}F NMR (C_6D_6, 470 MHz, 21°C): δ 56.5 (s, 1F, CF), -143.6 (dd, $^3J_{FF}$ = 25, $^5J_{FF}$ = 8 Hz, 2F, *o*-CF_2), -155.7 (td, $^3J_{FF}$ = 22, $^6J_{FF}$ = 6 Hz, 1F, *p*-CF), -163.1 (ddd, $^3J_{FF}$ = 25, $^3J_{FF}$ = 22, $^5J_{FF}$ = 8 Hz, 2F, *m*-CF_2).

Reaction of 12 with HCl.

Cp*(CO)Ir=$CFCF_3$ (80 mg, 0.17 mmol, isomer ratio 11:1, Z:E) was dissolved in toluene (4 mL) and an HCl-toluene solution (0.18 M, 1 mL, 0.18 mmol) was added at -78^{o}C. The dark yellow solution became lighter. NMR spectra of the crude solution showed formation of two diastereomers of the product, Cp*(CO)Ir($CHFCF_3$)(Cl) **19**, in an 11:1 ratio The solvent was evaporated under vacuum to give yellow solid (81 mg, 91%). The same procedure was repeated for starting material Z:E ratios of 6:1, 5:1, and 2:1 and the product showed 6:1, 5:1 and 2:1 diastereomer ratios respectively. Calcd for $C_{13}H_{16}ClF_4IrO$ (491.93): C, 31.74; H, 3.28. Found: C, 31.96; H, 3.64. IR: ν_{CO} = 2039 cm^{-1} (CH_2Cl_2). Major diatereomer: ^{1}H NMR (CD_2Cl_2, 500 MHz, 21^{o}C) δ 1.37 (s, C_5Me_5), 7.42 (dq, $^2J_{HF}$ = 47 Hz, $^3J_{HF}$ = 11 Hz, 1H, CHF). ^{19}F NMR (CD_2Cl_2, 470 MHz, 21^{o}C) δ -73.6 (dd, $^3J_{FF}$ = 15 Hz, $^3J_{H\,F}$= 11 Hz, 3F, CF_3), -194.7 (dq, $^2J_{HF}$ = 47 Hz, $^3J_{FF}$ = 15 Hz, 1F, CHF). Minor diastereomer: ^{1}H NMR (CD_2Cl_2, 500 MHz, 21^{o}C) δ1.24 (s, C_5Me_5), 6.23 (dq, $^2J_{HF}$ = 47 Hz, $^3J_{HF}$ = 10 Hz, 1H, CHF). ^{19}F NMR (CD_2Cl_2, 470 MHz, 21^{o}C) δ

-72.41 (dd, $^3J_{FF}$ = 15 Hz, $^3J_{HF}$ = 10 Hz, 3F, CF_3), -186.25(dq, $^2J_{HF}$ = 47 Hz, $^3J_{FF}$ = 15 Hz, 1F, CHF). Crystals of the major diastereomer were sent for X-ray diffraction. The specific crystal used for the diffraction experiment was returned and its NMR spectra confirmed to be of the major isomer, allowing idenification of the relative stereocehmistries of Ir and C in the major diasteromer to be confirmed.

Reaction of 13 with HCl.

The stereochemically pure carbene complex Cp*(PMe_3)Ir=$CFCF_3$ (0.023 g, 0.05 mmol, E isomer) was dissolved in toluene (5 mL) and cooled to -78°C. HCl-toluene (0.18 M, 0.3 mL, 0.05 mmol) was added at -78°C and the mixture was stirred (10 min). The solvent was evaporated under vacuum to give yellow solid product (0.021 g, 80%), shown to be a single diastereomer of Cp*(PMe_3)Ir($CHFCF_3$)(Cl) **20**, the stereochemistry of which has been characterized previously.[33] Reaction of a 4:1 (E:Z) mixture of starting material gave a 4:1 mixture of product diastereomers.

Reaction of 24 with HCl.

Cp*(CO)Ir=$C(CF_3)_2$ (37 mg, 0.073 mmol) was dissolved in toluene (10 mL). An HCl (1.25mL, 0.087 mmol, 0.07 M toluene solution) was added at -78°C. The ^{19}F NMR spectrum showed all of the starting material was converted to Cp*(CO)Ir(Cl)[$CH(CF_3)_2$] **25**. The solvent was removed to give a yellow solid product (39 mg, 99%). Calcd for $C_{14}H_{16}ClF_6IrO$ (541.94): C, 31.03; H, 2.98. Found: C, 30.92; H, 2.96. IR (hexane): ν(CO) = 2048 cm^{-1}. ^{1}H NMR (C_6D_6, 500 MHz, 21°C) δ 1.27 (s, 15H, C_5Me_5), 4.43 (septet, $^3J_{FH}$ = 12 Hz, 1H, IrCH). ^{19}F NMR (C_6D_6, 470 MHz, 21°C) δ -53.3 (dq, $^3J_{FH}$ =12 Hz, $^4J_{FF}$ = 10 Hz, 3F, CF_3), -56.0 (dq, $^3J_{FH}$ =12 Hz, $^4J_{FF}$ = 10 Hz, 3F, CF_3).

Reaction of 14 with HCl.

Cp*(CO)Ir=CFC_2F_5 (0.026 g, 0.0514 mmol, 3:1 ratio of Z:E isomers) was dissolved in toluene (8 mL) to give a bright yellow solution. This was cooled to -78°C, HCl in toluene (0.23M, 0.45 mL, 0.104

mmol) was added and the solution was stirred at -78°C (2 hours) before warming to room temperature. NMR spectra showed formation of product Cp*(CO)Ir($CFHCF_2CF_3$)(Cl) **21,** as a 3:1 ratio of diastereomers. The solvent was removed to give an analytically pure yellow solid. Anal. Calcd for $C_{14}H_{16}ClF_6IrO$ (541.92): C, 31.03; H, 2.98. Found: C, 31.37; H, 3.07. IR: ν_{CO} = 2042 cm^{-1} (hexanes). Major diastereomer: ^{1}H NMR (C_6D_6, 500 MHz, 21°C) δ 7.68 (ddd, $^2J_{HF}$ = 47, $^3J_{HF}$ = 30, $^3J_{HF}$ = 8 Hz, 1H, CFH), 1.40 (s, 15H, Cp*). ^{19}F NMR (C_6D_6, 470 MHz, 21°C) δ -81.88 (d, $^4J_{FF}$ = 13 Hz, 3F, CF_3), -114.8 (ddd, $^2J_{FF}$ = 275, $^3J_{FH}$ = 30, $^3J_{FF}$ = 17 Hz, 1F, CF_2), -115.6 (ddd, $^2J_{FF}$ = 275, $^3J_{FF}$ = 22, $^3J_{FH}$ = 8 Hz, 1F, CF_2), -196.3 (dddq, $^2J_{FH}$ = 47, $^3J_{FF}$ = 22, $^3J_{FF}$ = 17, $^4J_{FF}$ = 13 Hz, 1F, CFH). Minor diastereomer: ^{1}H NMR (C_6D_6, 500 MHz, 21°C) 7.46 (ddd, $^2J_{HF}$ = 47, $^3J_{HF}$ = 25, $^3J_{HF}$ = 10 Hz, 1H, CFH), 1.26 (s, 15H, Cp*). ^{19}F NMR (C_6D_6, 470 MHz, 21°C) δ -81.84 (d, $^4J_{FF}$ = 13 Hz, 3F, CF_3), -116.0 (ddd, $^2J_{FF}$ = 273, $^3J_{FF}$ = 21, $^3J_{FH}$ = 10 Hz, 1F, CF_2), -116.7 (ddd, $^2J_{FF}$ = 273, $^3J_{FH}$ = 25, $^3J_{FF}$ = 17 Hz, 1F, CF_2), -188.2 (dddq, $^2J_{FH}$ = 47, $^3J_{FF}$ = 21, $^3J_{FF}$ = 17, $^4J_{FF}$ = 13 Hz, 1F, CFH). Crystals of the major diastereomer were sent for X-ray diffraction. The specific crystal used for the diffraction experiment was returned and its NMR spectra confirmed to be of the major isomer, allowing idenification of the relative stereocehmistries of Ir and C in the major diasteromer to be confirmed.

Reaction of 15 with HCl.

Cp*(PMe_3)Ir=$CFCF_2CF_3$ (0.024 g, 0.043 mmol; 3:1 E:Z ratio) was dissolved in toluene (5 mL) and cooled to -78ºC to give a bright yellow solution. HCl/toluene (0.07M, 0.6 mL, 0.042 mmol) was added and the color became paler. NMR analysis showed the product to consist of a 3:1 mixture of diastereomers of Cp*(PMe_3)Ir($CFHCF_2CF_3$)(Cl) **22**, the stereochemistries of which have been characterized previously.[33] Reaction of a 4:1 (E:Z) mixture of starting material gave a 4:1 mixture of product diastereomers.

Reaction of 16 with HCl.

$Cp^*(CO)Ir{=}CFC_6F_5$ (0.086 g, 0.155 mmol; 5:1, Z:E ratio) was dissolved in toluene (5 mL) to give a bright yellow solution and cooled to -78ºC. HCl in toluene (0.07 M, 2.3 mL, 0.161 mmol) was added and the solution allowed to stir at -78ºC (30 min). NMR analysis showed the formation of the product $Cp^*(CO)Ir(CFHC_6F_5)(Cl)$ **23,** as a 5:1 mixture of diastereomers. Recrystallized from methylene chloride/hexanes yielded an analytically pure sample 0.055g (60%). Anal. Calcd for $C_{18}H_{16}ClF_6IrO$ (589.958): C, 36.64; H, 2.73. Found: C, 36.75; H, 2.61. IR: ν_{CO} (CH_2Cl_2) = 2032 cm^{-1}. Major diastereomer: ^1H NMR (C_6D_6, 500 MHz, 21°C): δ 7.07 (d, $^2J_{HF}$ = 49 Hz, 1H, CHF), 1.32 (s, 15H, Cp*). ^{19}F NMR (C_6D_6, 470 MHz, 21°C): δ -141.0 (td, $^4J_{FF}$ = 12, $^3J_{FF}$ = 8, 2F, *o*-F), -158.5 (td, $^3J_{FF}$ = 21, $^6J_{FF}$ = 2 Hz, 1F, *p*-F), -164.1 (dtd, $^2J_{HF}$ = 49, $^4J_{FF}$ = 12, $^6J_{FF}$ = 2 Hz, 1F, CHF), =164.9 (dt, $^3J_{FF}$ = 21, $^3J_{FF}$ = 8 Hz, 2F, *m*-F). Minor diastereomer: ^1H NMR (C_6D_6, 500 MHz, 21°C): δ 7.69 ($^2J_{HF}$ = 49 Hz, 1H, CHF), 1.20 (s, 15H, Cp*). ^{19}F NMR (C_6D_6, 470 MHz, 21°C): δ -141.2 (br s, 2F, *o*-F), -158.7 (td, $^3J_{FF}$ = 21, $^6J_{FF}$ = 2 Hz, 1F, *p*-F), -164.2 (dt, $^3J_{FF}$ = 21, $^3J_{FF}$ = 8 Hz, 2F, *m*-F), -170.5 (dt, $^2J_{HF}$ = 49, $^4J_{FF}$ = 11 Hz, 1F, CHF). Crystals of the major diastereomer were sent for X-ray diffraction. The specific crystal used for the diffraction experiment was returned and its NMR spectra confirmed to be of the major isomer, allowing idenification of the relative stereocehmistries of Ir and C in the major diasteromer to be confirmed.

General procedure for determination of isomerization kinetics

A known amount of $Cp^*(CO)Ir{=}CFR_F$ (5-10 mg) and an external standard, C_6F_6, was dissolved in a known amount of C_6D_6 (0.6-0.8 mL) and allowed to reach its photostationary composition under ambient light conditions.. ^1H and ^{19}F NMR spectra recorded. The NMR tubes were covered with aluminum foil and placed in an oil bath at a set temperature (30, 40, 47, 61ºC). NMR spectra were taken periodically until thermal equilibrium was reached. From the integration and the known concentration of the alkylidene in solution, the concentration of each isomer was determined at each time point. The difference between the initial concentration, $[A]_0$, and the concentration at time t was found and termed X. The difference between X at equilibrium, X_e, and X at time t was then calculated. A plot of the

natural log of (X_e-X) versus time (seconds) resulted in a line with slope equal to -(k_1+ k_{-1}). From this information and the known equilibrium constant, k_1 and k_{-1} were calculated. Plotting the ln of k/T versus 1/T (Eyring plot) for the rate constants determined at each temperature resulted in a line with slope equal to $-\Delta H^{\ddagger}/R$. The entropy of activation, $\Delta S^{\ddagger}$, was determined from the y-intercept using the equation, $y = \ln(k_B/h) + \Delta S^{\ddagger}/R$. Errors were found by determining the equations of the lines representing the two extremes of the error bars and calculating the respective $\Delta H^{\ddagger}$ and $\Delta S^{\ddagger}$ values.

X-ray Crystal Structure Determinations.

Diffraction intensity data were collected with Bruker Smart Apex CCD diffractometers. The structures were solved using the Patterson function, completed by subsequent difference Fourier syntheses, and refined by full matrix least-squares procedures on F^2. SADABS absorption corrections were applied to all structures. In all structures, all non-hydrogen atoms were refined with anisotropic displacement coefficients, and hydrogen atoms were treated as idealized contributions. All software and sources of scattering factors are contained in the SHELXTL (5.10) program package (G. Sheldrick, Bruker XRD, Madison, WI).

DFT calculations.

Calculations were carried out using the hybrid B3LYP functional[41-44] with the zero-damping, two-body only D3 correction of Grimme et al.,[45, 46] and the LACV3P**++ basis, which uses a pseudopotential for iridium,[47-50] and the 6-311++G** basis[63-66] for other atoms, as implemented in the Jaguar[67] suite of programs. Computed structures were confirmed as energy minima or transition states by calculating the vibrational frequencies using second derivative analytic methods, and confirming the absence of imaginary frequencies for minima and single imaginary frequency for transition states. Thermodynamic quantities were calculated assuming an ideal gas, and are zero point energy corrected.

Acknowledgment.

RPH is grateful to the U. S. National Science Foundation for generous financial support.

Electronic Supplementary Information Available

Details of all DFT calculated structures described herein. CCDC 1406693-1406699. For ESI and crystallographic data in CIF or other electronic format see DOI: 10.1039/x0xx00000x.

References

1. A. M. Rouhi, *Chem. Eng. News*, 2002, **80**, 29-33.
2. R. H. Grubbs, *Tetrahedron*, 2004, **60**, 7117-7140.
3. T. E. Taylor and M. B. Hall, *J. Am. Chem. Soc.*, 1984, **106**, 1576-1584.
4. G. Frenking, M. Sola and S. F. Vyboishchikov, *J. Organomet. Chem.*, 2005, **690**, 6178-6204.
5. I. Dalmazio and H. Anderson Duarte, *J. Chem. Phys.*, 2001, **115**, 1747-1756.
6. S. F. Vyboishchikov and G. Frenking, *Chem. Eur. J.*, 1998, **4**, 1428-1438.
7. R. H. Crabtree, *The Organometallic Chemistry of the Transition Metals*, John Wiley & Sons, Inc., New York, 1988.
8. R. P. Hughes, *Adv. Organomet. Chem.*, 1990, **31**, 183-267.
9. R. P. Hughes, *J. Fluor. Chem.*, 2010, **131**, 1059-1070.
10. P. J. Brothers and W. R. Roper, *Chem. Rev.*, 1988, **88**, 1293-1326.
11. B. E. Smart, in *Chemistry of Functional Groups, Supplement D*, eds. S. Patai and Z. Rappoport, Wiley, New York, 1983, vol. 1, pp. 603-655.
12. K. B. Wiberg and P. R. Rablen, *J. Am. Chem. Soc.*, 1993, **115**, 614-625.
13. D. A. Dixon, T. Fukunaga and B. E. Smart, *J. Am. Chem. Soc.*, 1986, **108**, 4027-4031.
14. A. E. Reed and P. v. R. Schleyer, *J. Am. Chem. Soc.*, 1990, **112**, 1434-1445.
15. M. M. Rahman, D. M. Lemal and W. P. Dailey, *J. Am. Chem. Soc.*, 1988, **110**, 1964-1966.
16. J. G. Stamper and R. Taylor, *Journal of Chemical Research, Synopses*, 1980, 128.
17. D. L. S. Brahms and W. P. Dailey, *Chem. Rev.*, 1996, **96**, 1585-1632.
18. S. Koda, *Chem. Phys.*, 1982, **66**, 383-390.
19. S. Koda, *Chem. Phys. Lett.*, 1978, **55**, 353-357.
20. D. A. Dixon, *J. Phys. Chem.*, 1986, **90**, 54-56.
21. E. Bleuel, P. Schwab, M. Laubender and H. Werner, *J. Chem. Soc., Dalton Trans.*, 2001, 266-273.
22. D. A. Ortmann, B. Weberndörfer, K. Ilg, M. Laubender and H. Werner, *Organometallics*, 2002, **21**, 2369-2381.
23. C. P. Casey, P. C. Vosejpka and F. R. Askham, *J. Am. Chem. Soc.*, 1990, **112**, 3713-3715.
24. C. P. Casey, H. Sakaba and T. L. Underiner, *J. Am. Chem. Soc.*, 1991, **113**, 6673-6674.
25. C. P. Casey, C. J. Czerwinski, D. R. Powell and R. K. Hayashi, *J. Am. Chem. Soc.*, 1997, **119**, 5750-5751.
26. G. R. Clark, S. V. Hoskins, T. C. Jones and W. R. Roper, *J. Chem. Soc., Chem. Commun.*, 1983, 719-721.
27. A. K. Burrell, G. R. Clark, J. G. Jeffrey, C. E. F. Rickard and W. R. Roper, *J. Organomet. Chem.*, 1990, **388**, 391-408.
28. R. P. Hughes, R. B. Laritchev, J. Yuan, J. A. Golen, A. N. Rucker and A. L. Rheingold, *J. Am. Chem. Soc.*, 2005, **127**, 15020-15021.

29. D. L. Reger and M. D. Dukes, *J. Organomet. Chem.*, 1978, **153**, 67-72.
30. J. D. Koola and D. M. Roddick, *Organometallics*, 1991, **10**, 591-597.
31. R. P. Hughes and J. M. Smith, *J. Am. Chem. Soc.*, 1999, **121**, 6084-6085.
32. R. P. Hughes, D. Zhang, L. N. Zakharov and A. L. Rheingold, *Organometallics*, 2002, **21**, 4902-4904.
33. S. A. Garratt, R. P. Hughes, I. Kovacik, A. J. Ward, S. Willemsen and D. Zhang, *J. Am. Chem. Soc.*, 2005, **127**, 15585-15594.
34. R. P. Hughes, R. B. Laritchev, L. N. Zakharov and A. L. Rheingold, *J. Am. Chem. Soc.*, 2005, **127**, 6325-6334.
35. R. P. Hughes, S. Willemsen, A. Williamson and D. Zhang, *Organometallics*, 2002, **21**, 3085-3087.
36. H. Berke and R. Hoffmann, *J. Am. Chem. Soc.*, 1978, **100**, 7224-7236.
37. C. J. Bourgeois, R. P. Hughes, J. Yuan, A. G. DiPasquale and A. L. Rheingold, *Organometallics*, 2006, **25**, 2908-2910.
38. D. J. Harrison, G. M. Lee, M. C. Leclerc, I. Korobkov and R. T. Baker, *J. Am. Chem. Soc.*, 2013, **135**, 18296-18299.
39. D. J. Harrison, S. I. Gorelsky, G. M. Lee, I. Korobkov and R. T. Baker, *Organometallics*, 2012, **32**, 12-15.
40. M. P. Andersson and P. Uvdal, *J. Phys. Chem. A*, 2005, **109**, 2937-2941.
41. P. J. Stephens, F. J. Devlin, C. F. Chabalowski and M. J. Frisch, *J. Phys. Chem.*, 1994, **98**, 11623-11627.
42. A. D. Becke, *J. Chem. Phys.*, 1993, **98**, 1372-1377.
43. A. D. Becke, *J. Chem. Phys.*, 1993, **98**, 5648-5652.
44. C. Lee, W. Yang and R. G. Parr, *Phys. Rev. B*, 1988, **37**, 785-789.
45. L. Goerigk and S. Grimme, *Phys. Chem. Chem. Phys.*, 2011, **13**, 6670-6688.
46. S. Grimme, J. Antony, S. Ehrlich and H. Krieg, *J. Chem. Phys.*, 2010, **132**, 154104.
47. W. R. Wadt and P. J. Hay, *J. Chem. Phys.*, 1985, **82**, 284-298.
48. P. J. Hay and W. R. Wadt, *J. Chem. Phys.*, 1985, **82**, 299-310.
49. P. J. Hay and W. R. Wadt, *J. Chem. Phys.*, 1985, **82**, 270-283.
50. T. H. Dunning and P. J. Hay, eds., *Modern Theoretical Chemistry, Vol. 4: Applications of Electronic Structure Theory*, Plenum, NY, 1977.
51. R. P. Hughes, J. M. Smith, L. M. Liable-Sands, T. E. Concolino, K.-C. Lam, C. Incarvito and A. L. Rheingold, *J. Chem. Soc. Dalton Trans.*, 2000, 873-879.
52. A. M. Crespi and D. F. Shriver, *Organometallics*, 1985, **4**, 1830-1835.
53. R. P. Hughes, R. B. Laritchev, A. Williamson, C. D. Incarvito, L. N. Zakharov and A. L. Rheingold, *Organometallics*, 2003, **22**, 2134-2141.
54. D. D. Callander, P. L. Coe, M. F. S. Matough, E. F. Mooney, A. J. Uff and P. H. Winson, *Chem. Comm.*, 1966, **22**, 820-821.
55. R. P. Hughes, D. Zhang, A. J. Ward, L. N. Zakharov and A. L. Rheingold, *J. Am. Chem. Soc.*, 2004, **126**, 6169-6178.
56. Saltiel, J.; D'Agostino, J.; Megarity, E. D.; Metts, L.; Neuberger, K. R.; Wrighton, M.; Zafiriou, O. C. In "Organic Photochemistry"; Chapman, O. L., Ed.; Marcel Dekker: New York, 1973; Vol. 3, pp.1-113
57. F. B. McCormick, W. A. Kiel and J. A. Gladysz, *Organometallics*, 1982, **1**, 405-408.
58. Raff, L. M. Principles of Physical Chemistry, Prentice Hall: Upper Saddle River, NJ, 2001.
59. J. Yuan, R. P. Hughes and A. L. Rheingold, *Eur. J. Inorg. Chem.*, 2007, 4723-4725.
60. A. B. Pangborn, M. A. Giardello, R. H. Grubbs, R. K. Rosen and F. J. Timmers, *Organometallics*, 1996, **15**, 1518-1520.
61. R. Csuk, *Nachrichten aus Chemie, Technik und Laboratorium*, 1987, **35**, 828-833.
62. R. Csuk, B. I. Glaenzer and A. Furstner, *Adv. Organomet. Chem.*, 1988, **28**, 85-137.
63. M. J. Frisch, J. A. Pople and J. S. Binkley, *J. Chem. Phys.*, 1984, **80**, 3265-3269.

64. T. Clark, J. Chandrasekhar, G. W. Spitznagel and P. v. R. Schleyer, *J. Comput. Chem.*, 1983, **4**, 294-301.
65. A. D. McLean and G. S. Chandler, *J, Chem. Phys.*, 1980, **72**, 5639-5648.
66. R. Krishnan, J. S. Binkley, R. Seeger and J. A. Pople, *J. Chem. Phys.*, 1980, **72**, 650-654.
67. Schrödinger, LLC, New York, NY, Jaguar, versions 7.0-8.3, 2007-2014.